



Recycling for Recovery of Critical Metals from LiCoO₂ Cathode Material Through Methanesulfonic Acid-Citric Acid Organic Leaching System

Jae-Yeon Kim^{1,2} · Jiajia Wu³ · Eun-Woo Kim⁴ · Yoo-Jin Kim⁴ · Jun-Jae Lee⁴ · Jai-Won Byeon⁴ · Junmo Ahn⁵ · Jaeheon Lee^{1,2}

Received: 3 March 2023 / Accepted: 15 August 2023 / Published online: 20 September 2023
© Society for Mining, Metallurgy & Exploration Inc. 2023

Abstract

Growing demand for valuable battery materials and environmental issues from battery disposal make the recycling of spent lithium-ion batteries (LIBs) essential. Specifically, the green approaches using organic reagents have garnered many attentions for battery recycling. In this study, a synergetic organic leaching system using methanesulfonic acid (MSA) of strong organic acid and citric acid (CA) with good chelating ability was investigated to extract valuable metals from LiCoO₂. Hydrogen peroxide was used as a reducing agent to enhance leaching kinetics. Cobalt extraction of 98% and lithium extraction of 97 % were achieved in the optimized condition; 2.4M MSA, 1.6M CA, 1.0 vol% H₂O₂, S/L ratio 80 g/L, 85 °C, and 1 h. The optimal leaching condition of the MSA-CA mixed leaching system exhibited good applicability to various cathode scraps, such as LiCoO₂, LiNi_xMn_yCo_{1-x-y}O₂, and LiNi_xCo_yO₂. The dissolved Co and Li ions in the MSA-CA leachate were selectively recovered with high recovery efficiencies of 99 % and 97 % as Co₃O₄ and Li₃PO₄, respectively. The recovered Co₃O₄ and Li₃PO₄ were utilized to regenerate cathode materials. LiCoO₂ and LiFePO₄ were also synthesized through a solid-state reaction and hydrothermal method. The recycling process based on the MSA-CA-H₂O₂ synergetic leaching system was proposed, and it might be applied as a green and economical organic leaching system for the recycling of various types of spent LIBs.

Keywords Methanesulfonic acid · Citric acid · Spent lithium-ion batteries · Leaching · Recycling

1 Introduction

Rechargeable lithium-ion batteries (LIBs) have been used as clean energy sources for electric vehicles to reduce greenhouse gas emissions [1, 2]. Accordingly, the demand for valuable metals used as cathode materials has grown increasingly. Nowadays, because of the depletion of primary

resources, recycling critical metals from secondary resources has become a vital strategy to address the regional metal deficiency, maximize resource utilization efficiency, and minimize the hazardous environmental influence of waste disposal [3–5]. Regarding LIB recycling, the estimated current rate of second-life battery supply is approximately one gigawatt-hours per year. However, the second-life battery supply for EVs could increase by 200 gigawatt-hours per year by 2030. A global market with a value north of \$30 billion will be expected to be constituted by 2030 [6].

Pyro-, hydro-, and bio-metallurgical approaches have been considered to recycle valuable metals from the spent LIBs. Currently, the hydrometallurgical method has been widely applied in many LIBs recycling companies such as Duesenfeld (Germany), Umicore (Belgium), Li-Cycle (USA), and SungEel HiTech (Republic of Korea) [7, 8] because critical metals of high purity can be recovered, and it is more energy-efficient and eco-friendly than the pyro- and bio-metallurgical approaches [9]. Hydrometallurgical processes consist of three stage processes: (1) metal dissolution by leaching processes; (2) concentration and

✉ Jaeheon Lee
jaecheonlee@mines.edu

¹ Department of Mining Engineering, Colorado School of Mines, Golden, CO 80401, USA

² Kroll Institute for Extractive Metallurgy, Colorado School of Mines, Golden, CO 80401, USA

³ School of Mineral Processing and Bioengineering, Central South University, Changsha 410083, China

⁴ Material Science and Engineering, Seoul National University of Science and Technology, Seoul 01811, Republic of Korea

⁵ Department of Mineral Resources and Energy Engineering, Chonbuk National University, Jeonju-si, Jeollabuk-do 54896, Republic of Korea

purification by solvent extraction, ion exchange, or cementation; and (3) metal recovery by precipitation or electrolysis. In the hydrometallurgical processes for the LIB recycle, the leaching processes are mostly conducted using mineral acids with strong acidity (i.e., low dissociation constant, pK_a) [10]. Among the mineral acids, sulfuric acid (H_2SO_4) has been utilized commercially due to its low cost and low corrosiveness to industrial facilities [11, 12]. In addition, reducing agents, such as H_2O_2 , $Na_2S_2O_5$, and $NaHSO_3$ are added to improve the leaching kinetics of cathode materials [13].

In this context, organic acids are attracting attention as eco-friendly alternatives to mineral acids [9]. Mineral acids of HCl , HNO_3 , and H_2SO_4 inevitably produced toxic by-products such as Cl_2 , NO_x , and SO_x in the leaching processes [14]. On the other hand, various organic acids are less toxic than mineral acids due to the following reasons: (1) mild acidity relative to mineral acids; (2) biodegradability characteristics; and (3) organic acids mainly consist of C, H, and O atoms; thus, toxic by-products are not produced during the leaching [9]. A variety of organic acids have been explored to dissolve cathode scraps, such as lactic acid ($C_3H_6O_3$), succinic acid ($C_4H_6O_4$), malic acid ($C_4H_6O_5$), tartaric acid ($C_4H_6O_6$), benzenesulfonic acid ($C_6H_6O_3S$), ascorbic acid ($C_6H_8O_6$), and citric acid ($C_6H_8O_7$) [15–19]. Furthermore, several organic chemicals have been investigated as reducing agents to apply for cathode material leaching, for example, H_2SO_4 -ascorbic acid [13], H_3PO_4 -glucose [20], maleic acid-grape seed extract [21], citric acid-orange peel extract [22], and citric acid-tea waste [23]. However, an extended leaching time with an elevated leaching temperature and a low S/L ratio of organic leaching systems compared to the mineral acid leaching system has limited their industrial applications.

To overcome those disadvantages of organic leaching systems, synergetic organic leaching systems using mixed organic lixiviant have been of particular interest. Generally, in the organic leaching system, valuable metals for cathode materials are leached through acidolysis and complexolysis phenomena [24]. The mixed organic lixiviants consist of organic chemicals with either strong acidity (i.e., lower pK_a) or good complexing ability, and it may be a practical approach to improve the leaching performance by using the synergistical system as well as to achieve a green process. There have been a few studies on the mixed organic leaching system for cathode materials, such as citric acid-salicylic acid- H_2O_2 [25], citric acid-glucose [26], citric acid-ascorbic acid [27], benzenesulfonic acid and formic acid [28], and tartaric acid-citric acid-ascorbic acid systems [29]. In those studies, H_2O_2 , glucose, ascorbic acid, and formic acid were used as reducing agents. The mixed organic leaching systems were effective for the leaching of the cathode materials, but their reagent cost was still more expensive than that of the conventional inorganic acids. A thorough economic

analysis should be performed before considering the system for industrial implementation.

Among various organic acids, methanesulfonic acid (MSA, CH_3SO_3) with the lowest pK_a value could be one of the most suitable organic acid responsible for the acidolysis mechanism for the mixed organic leaching system. Recently, MSA has exhibited broad applicability in hydrometallurgical processes as a promising sustainable organic lixiviant due to its advantages: (1) a high solubility of metals, (2) a strong acidity with a significantly lower pK_a value (−1.9) compared to other organic acids, and (3) a biodegradability [30–33]. The applicability of MSA for the lithium cobalt oxide (LCO, $LiCoO_2$) leaching with the H_2O_2 as a reductant was investigated [14]. It was reported that 5M MSA-5vol% H_2O_2 system achieved a leaching efficiency of 92.4 % Co and nearly 100% Li at 163 g/L for pulp density. Meanwhile, citric acid (CA) might be used as an agent for complexolysis and reductant due to its polyproticity, relatively low pK_a (i.e., pK_{a1} : 3.13, pK_{a2} : 4.76, pK_{a3} : 6.40) and good complexing ability with valuable metals [9]. In addition, its waste liquids can be easily decomposed in an anaerobic and aerobic environment [34]. Above mentioned, there were some reports on the mixed leaching system, but, a new green leaching system coupled with MSA for LCO recycling has not been reported until now.

After leaching, the dissolved metals in the leached solution are recovered as cobalt oxalate (CoC_2O_4), cobalt hydroxide ($Co(OH)_2$), lithium carbonate (Li_2CO_3), or lithium phosphate (Li_3PO_4) through precipitation processes [35]. Although the precipitation processes to recover Co and Li from leached solution by H_2SO_4 and some organic acids are well known, the optimized conditions for recovering Co from the leachate may depend on the leaching system as presented in Table S1 of supporting materials. In the case of the organic leaching system, the conditions for the precipitation process are believed to notably depend on the type of organic acids because the organics can form complexes with either Co or Li ions and the complexation behavior depends on the chemicals. Thus, optimization of process parameters for recovering Co or Li ions from the MSA-CA mixed organic leaching system, which would be studied in this study, necessarily is required.

MSA-CA mixed leaching system was investigated as a whole green leaching process to achieve the effective dissolution of cathode materials. Wu [36] previously optimized the lixiviant ratio, lixiviant concentration, and solid/liquid (S/L) ratio of the MSA-CA leaching system. In this study, the effect of H_2O_2 was investigated to enhance the reaction kinetic of the MSA-CA leaching system. The leaching performance and economic feasibility of this leaching system in terms of reagent and electricity cost for the leaching test were compared to various organic acids and the H_2SO_4 as a conventional lixiviant. The optimal

operating condition of the MSA-CA-H₂O₂ leaching system was applied to various cathode scraps from spent LIBs for the sake of examination of its diverse applicability. The dissolved Co and Li in the leachate were recovered into Co₃O₄ and Li₃PO₄ as the cathode precursors. Subsequently, by utilizing the recovered Co₃O₄ and Li₃PO₄, LCO and lithium iron phosphate (LFP, LiFePO₄) were regenerated via solid-state reaction and hydrothermal synthetic method, respectively.

2 Materials and Experimental Methods

2.1 Materials

A leaching test was conducted using synthetic LCO powder of 97% purity (Alfa Aesar) to optimize leaching conditions. Compositions of synthetic LCO are 6.87 Li wt% and 58.4 Co wt%. Afterward, to validate the applicability of the mixed leaching system, secondary leaching tests using synthetic MNC 622 powder (MSE suppliesTM) and cathode scraps from spent LIBs were conducted at the optimized conditions. Compositions of synthetic NMC 622 are 7.13 Li wt%, 58.8 Ni+Mn+Co wt%, Na 0.0118 wt %, 0.0004 wt%, and 0.0001 Cu wt%. The LCO, lithium nickel cobalt oxide (NCO), and lithium nickel manganese cobalt oxide (NMC) cathode scraps were provided by SungEel HiTech. Co., Ltd (Korea). Spent batteries were mechanically broken by a shredder after discharging. And then, several separation processes, such as magnetic separation, electrostatic separation, and sieving separation, were applied to shredded spent batteries to remove impurities. Scraps under 200 mesh were used for leaching tests. Its chemical compositions analyzed by inductively coupled plasma-optical emission spectrometry (ICP-OES) following aqua regia digestion were in Table 1. And, their phases analyzed by X-ray diffraction (XRD) were summarized in Table 2.

Table 1 Compositions of spent battery scraps, which were analyzed by ICP-OES

Element (wt%)	LCO scrap 1	LCO scrap 2	NMC scrap	NCO scrap
Al	3.92	<0.1 %	4.70	0.56
Co	21.63	54.60	3.88	6.59
Cu	1.27	0.01	6.86	0.00
Fe	0.03	0.02	1.25	0.47
Li	2.29	6.46	3.36	6.55
Mn	0.06	0.13	1.49	0.57
Ni	0.21	0.63	16.88	42.39

Table 2 Phase of spent battery scraps, which were analyzed by XRD

Phase	LCO scrap 1	LCO scrap 2	NMC scrap	NCO scrap
Graphite	76.5	-		68.0
Li(Co,Ni,Mn) O ₂	4.7	100	100	2.4
CoO	13.1	-		0.0
Cuprite	1.6	-		6.7
Nickel	0.0	-		6.9
Aluminum	1.0	-		6.1
LiAlO ₂	0.0	-		5.0
Tenorite	0.6	-		2.3
NiO ₂	0.0	-		2.0
Cobalt	1.0	-		0.0
Goethite	0.7	-		0.7
CoO ₂	0.8	-		0.0

2.2 Leaching Test

The leaching test was conducted using a 1L reactor which was covered by a vessel lid to prevent the evaporative loss of the solution. The temperature of solution was controlled up to 85 °C by using a water bath and circulator. The organic leaching solution composed of MSA (99% extra pure, Acros Organics) and CA (99.5% citric acid anhydrous, certified ACS, Fisher Chemical) was prepared prior to the leaching test. The concentrations of MSA and CA were 2.4 M and 1.6 M, respectively. After the solution temperature was reached the set temperature, 16 g sample was added into the 200 mL solution to achieve a primary S/L ratio of 80 g/L. H₂O₂ of 0.5–4.5 vol% (30 %, Certified ACS, Fisher Chemical) was added to the leaching solution as a reductant. The leaching reactor was agitated using a magnetic stir bar. Kinetic samples were taken at several intervals, and the concentrations of dissolved elements were analyzed through atomic absorption spectrometry (AAS, PinAAcle 900F, PerkinElmer, UK). The calculation formula for the leaching efficiency is presented as follows (Eq. (1)):

$$R = \frac{c \cdot V}{m \cdot w} \times 100 \quad (1)$$

where R is leaching efficiency (%), c is metal concentration in leaching solution (g/L), V is solution volume (L), m is sample weight (g), and w is the weight percent of the metal in the sample (wt%).

2.3 Co and Li Recovery from Leachate and Regeneration of Cathode Materials

Cobalt in the LCO leachate were recovered into cobalt oxalate (CoC₂O₄) by precipitation process using oxalic acid (OA, C₂H₂O₄·2H₂O, certified ACS, Fisher Chemical). For

the sake of the precipitation of CoC_2O_4 , an initial pH and temperature of the leachate were 2 and 25°C. The pH was controlled by 10 M NaOH (certified ACS, Fisher Chemical) and was measured using Orion star A221 pH meter (Thermo Scientific, US). And then, 3M OA solution of 65°C was added in the leachate with the 1:1.2 molar ratio between oxalate ($\text{C}_2\text{O}_4^{2-}$) and Co^{2+} in solution. The precipitation reaction was conducted for 1 h. The pink-colored CoC_2O_4 precipitates were collected by filtration, washed with distilled water, and then dried. The precipitates were calcinated in a muffle furnace at 400 °C for 6 h to generate the Co_3O_4 compound. For the sake of regeneration of LCO cathode via a solid-state reaction, the recovered Co_3O_4 and commercial Li_2CO_3 (ACS reagent, Sigma-Aldrich) was homogeneously mixed with a Li/Co molar ratio of 1:1 in ball mill at 300 rpm for 2 h. The mixture was sintered in a muffle furnace at 800 °C for 15 h in air atmosphere. The heating rate was 10°C/min.

The Li ions remained in the leachate after the Co precipitation process were recovered into the Li_3PO_4 compound via precipitation process using sodium phosphate (Na_2HPO_4 , 99 %, Sigma-Aldrich). Before Li recovery, the initial pH of leachate was adjusted between 9 and 12 using 10 M NaOH. Subsequently, 0.7 M Na_2HPO_4 was added into the leachate with the 1:3 molar ratio between PO_4^{3-} and Li^+ in the solution. The pH of 0.7M Na_2HPO_4 was also adjusted between 9 and 12 corresponding to that of leachate pH before adding into the leachate. The reaction was conducted for 30 min. The filtered light blue Li_3PO_4 powders were thoroughly washed with distilled water at 50 °C and dried in the oven. The recovered Li_3PO_4 was utilized to synthesize the LFP cathode materials through the hydrothermal method. Firstly, $\text{FeSO}_4 \cdot 7\text{H}_2\text{O}$ (99.5%, Sigma-Aldrich) and 10 wt% ascorbic acids were dissolved in 40 mL of deionized water. And then, the recovered Li_3PO_4 was slowly dispersed into the FeSO_4 solution under stirring. The ratio of $\text{Li}_3\text{PO}_4/\text{FeSO}_4$ was 1:1 and the final concentration of FeSO_4 was controlled to 0.2 M. After sufficient mixing, the prepared mixture was transferred to the hydrothermal synthesis reactor and heated at 180°C for 10 h. After cooling down to room temperature, the obtained products were filtered and washed by deionized water.

2.4 Material Characterizations

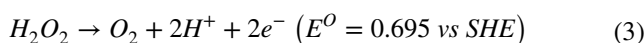
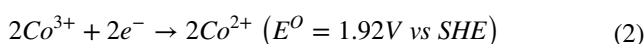
The crystal phases of the recovered materials were analyzed by X-ray diffractometer (XRD, SU8010, Hitachi, Japan) with the scan rate of 2°/min using Cu-K alpha as a source of X-rays. Their morphologies were observed with a scanning electron microscope (SEM, JSM-6700A, JEOL LTD., Japan). Energy dispersive X-ray spectroscopy (EDS) and ASS were used to identify the impurity of the recovered materials. Before the impurities of samples were analyzed with ASS, the samples were fully dissolved into aqua regia at 60 °C.

3 Results and Discussion

3.1 Effect of H_2O_2 on the Leaching of Synthetic LCO

Figure 1 (a) and (b) shows the effect of the molar ratio between MSA and CA on the Co and Li leaching efficiencies. The total molar concentration of organic acids was set at 1M. Compared to the only 1M CA or 1M MSA condition, the hybrid solutions tended to exhibit better leaching efficiencies. The MSA:CA molar ratio of 3:2 was the optimized condition for the leaching of synthetic LCO, where the Co and Li leaching efficiencies were 85 % and 81 %, respectively. This result indicated that the hybrid organic leaching system synergistically affected Co and Li dissolution from the LCO. Meanwhile, the leaching kinetics of Co was slower than that of Li. Li in LCO exists as soluble Li^+ . Li can easily undergo oxidation in most acidic solutions. On the other hand, Co in LCO exists as insoluble Co^{3+} , making it relatively difficult to dissolve in any acidic solutions unless properly reduced.

To improve the reaction kinetic in MSA-CA mixed leaching system, H_2O_2 was added as a reductant. The basic conditions for synthetic LCO leaching were follows: 2.4M MSA, 1.6M CA, S/L ratio 80 g/L, and 85°C, which were optimized in prior research [36]. Figure 1 (c) and (d) shows the effect of H_2O_2 concentrations on the Co and Li extraction from synthetic LCO. The concentrations of H_2O_2 were 0, 0.5, 1, 1.5, 3, and 4.5 vol%. The molar ratios of H_2O_2 to LCO at each H_2O_2 vol% can be expressed to 0, 0.26, 0.52, 0.78, 1.56, and 2.34. The leaching rates of LCO, particularly Co, were notably improved by adding a small amount of 1.0 vol% H_2O_2 (the molar ratios of H_2O_2 to LCO: 0.52). The leaching efficiencies of Co and Li in the presence of H_2O_2 above 1.0 vol% reached to 90 % and 91 % within around 1 hr. Figure 1 (e) shows the Co and Li extraction efficiencies with the H_2O_2 concentration after the leaching for only 1 h. The leaching efficiencies of Co and Li were increased rapidly to approximately 90 % with increasing the H_2O_2 concentration to 1 vol%. However, above 1 vol % H_2O_2 , the efficiencies increased much slower. H_2O_2 with a strong reducing ability can destabilize the LCO structure by reducing insoluble Co^{3+} into soluble Co^{2+} species [14, 23]. The reduction of Co^{3+} by H_2O_2 could be described according to the following equation (Eqs. (2) and (3)) [37]:



Due to the collapsed LCO structure, the leaching process could be accelerated by MSA and CA. However, the addition of a large amount of H_2O_2 above 1.0 vol% showed a negligible effect on the overall leaching efficiency. The result might

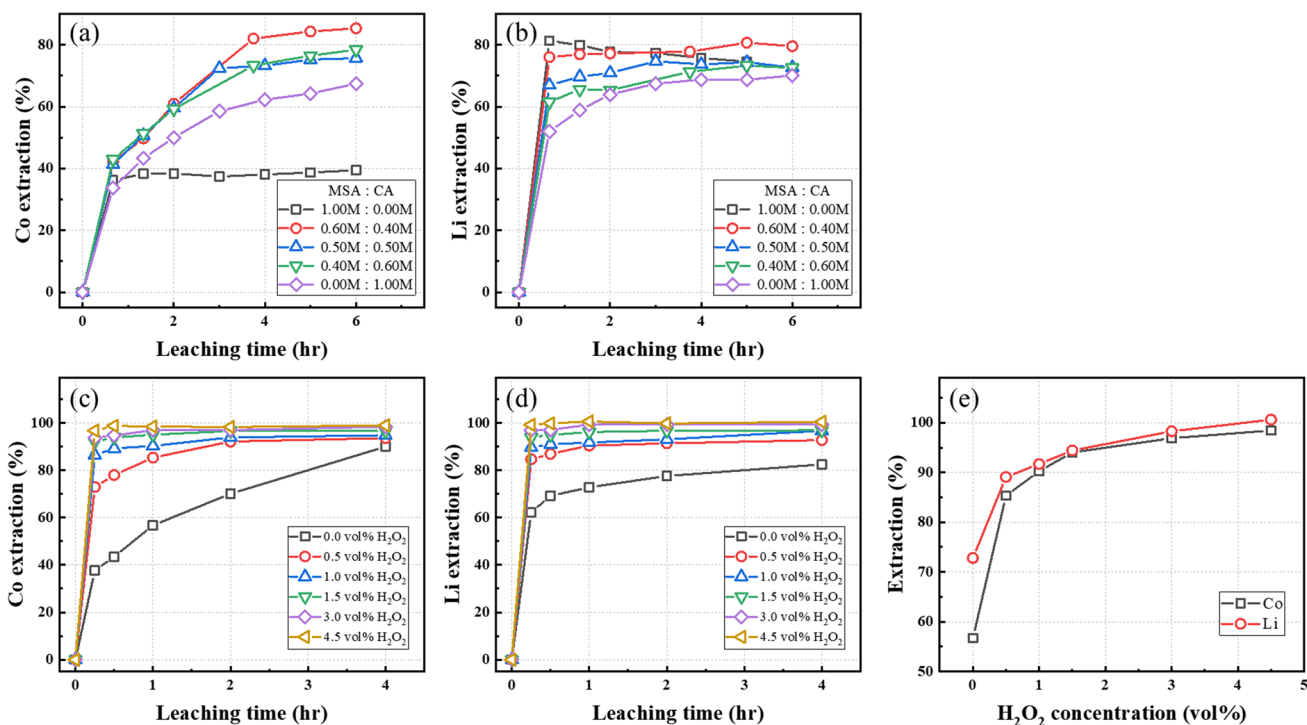
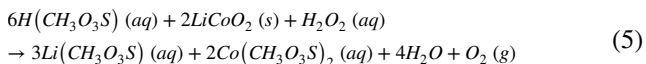
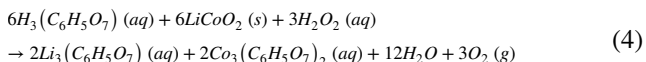


Fig. 1 Effect of molar ratio between MSA and CA on **a** Co and **b** Li leaching from the LCO powder. The leaching conditions of **(a, b)** were as follows: 80 g/L S/L ratio and 85°C. Effect of H₂O₂ concentration on **c** Co and **d** Li leaching from the LCO powder. The leaching

conditions of **(c–e)** were as follows: 2.4 MSA, 1.6 CA, 80 g/L S/L ratio, 85°C. **e** Co and Li extraction efficiencies at 1 hr with increasing the H₂O₂ concentration, which is from **(c)** and **(d)**

be because a large portion of H₂O₂ were easily decomposed at the high temperature of 85°C when a large amount of H₂O₂ were added at once. In this study, the overall leaching reactions were described as below:



The molar ratios of H₂O₂ to LCO based on Eqs. (4) and (5) were 0.5. In Fig. 1 (c) and (d), the optimized H₂O₂ consumption for the LCO leaching in the MSA and CA leaching system was 1 vol%, where the molar ratio of H₂O₂ to LCO is 0.52. This result shows that the reaction stoichiometry for the experimental results is well matched with the leaching reaction equation.

To minimize the consumption of H₂O₂ due to the decomposition during the leaching, 1 vol% H₂O₂ was separately added in the solution when the leaching test was started and after 30 min. Figure 2 shows the results for the effect of two separate additions of H₂O₂ on the LCO leaching. The Co and Li extraction efficiencies were improved up to 98 % and 97 % within 1 h by the separate additions of

H₂O₂. Thus, the optimized conditions for the 2.4M MSA-1.6M CA mixed leaching system were concluded to be the leaching time for 1 h at 85°C and the separate addition of 1 vol% H₂O₂.

3.2 Effect of Temperature and Leaching Kinetics

Figure 3 presents the changes of Co and Li extraction efficiencies using 2.4M MSA-1.6M CA leaching system from 30 to 85°C. The Co and Li extraction efficiencies and leaching kinetics were enhanced with increasing the reaction temperature. Maximum extraction of both metals was observed at 85°C. To determine the rate-controlling step for the leaching of metals from the LCO cathode scraps, the experimental data were analyzed on the basis of the shrinking core model. Leaching of metals from the cathode scraps could be a solid-liquid heterogeneous reaction, and it conforms to the unreacted shrinking core model [38]. Thus, the leaching kinetics are basically controlled by an ash or product layer diffusion control, a surface chemical reaction, or a diffusion through a fluid film. Meanwhile, several researchers discussed that LCO might be continuously dissolved without the formation of solid phase during the leaching process, which implies that the process of LCO dissolution in acidic solutions can be regarded as a reverse process of crystallization [38, 39].

Fig. 2 Effect of two separating addition of 1 vol% H₂O₂ on **a** Co and **b** Li leaching from the LCO powder. The leaching conditions were follows: 2.4 MSA, 1.6 CA, 80 g/L S/L ratio, 85 °C

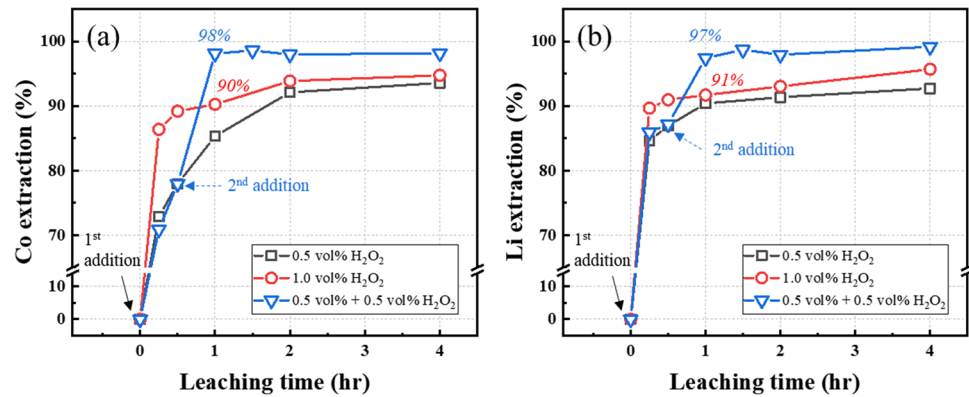
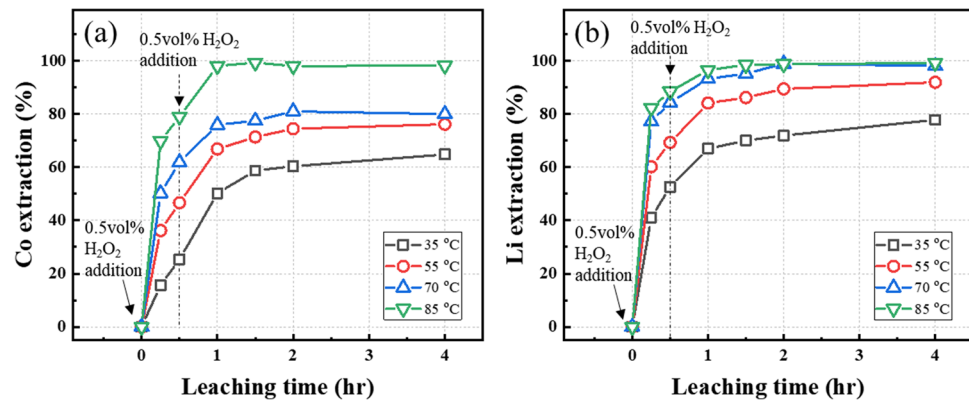


Fig. 3 Effect of the temperature on **a** Co and **b** Li leaching from the LCO powder. The leaching conditions were follows: 2.4 MSA, 1.6 CA, 80 g/L S/L ratio, the separate addition of 1 vol% H₂O₂



Furthermore, the LCO leaching is the multi-metals leaching of solid-liquid reactions. In this case, it has been reported that Avrami equation may be successfully employed to explain the leaching kinetics [38, 39]. The Avrami equation is expressed as Eq. (6):

$$\ln(-\ln(1-x)) = \ln k + n \ln t \quad (6)$$

where x is fraction of metal extraction, k is rate constant (h^{-1}), t is leaching time (h). Figure 4 (a–h) shows the linear fitting results based on four leaching kinetic models. By referring to R^2 values, the Avrami equation model had a pertinent fitting correlation with LCO leaching process than the other three models, indicating LCO leaching process in MSA-CA system could be well-explained via the Avrami equation. According to Sokić's report [40], the leaching process is limited by the surface chemical-controlled reaction when the n value in the Avrami equation is above 0.5. The n values for Co and Li at 85 °C, which is the optimal leaching condition, were 0.850 and 0.504, respectively. This result shows that the leaching process at 85 °C in the 2.4M MSA-1.6M CA-1 vol% H₂O₂ was limited by the surface chemical-controlled reaction.

The relationship between the reaction rate constant and the leaching temperature can be explained by the Arrhenius law as presented in Eq. (7):

$$k = Ae^{-E_a/RT} \quad (7)$$

where k is the reaction constant (h^{-1}), A is the frequency factor, E_a is the apparent activation energy (kJ/mol), R is the universal gas constant (8.314 J/mol·K), and T is the absolute temperature (K). Figure 5 (a) and (b) presents the Arrhenius plot of Co and Li. The calculated activation energy of Co and Li was 30.58 kJ/mol and 23.11 kJ/mol, respectively. When the apparent activation energy for a reaction is higher than 42 kJ/mol, the chemical reaction controls the overall reaction. In this case, the formation and breaking of chemical bonds become the rate-determining steps. When the apparent activation energy is lower than 18 kJ/mol, the reaction rate is mainly influenced by the diffusion of reactant molecules. In this case, the rate-determining step is the diffusion of reactant molecules to the reaction site. When the apparent activation energy falls between the ranges of 18 and 42 kJ/mol, both chemical reaction control and diffusion control can play a significant role in determining the overall reaction rate. In this case, the rate of the reaction is

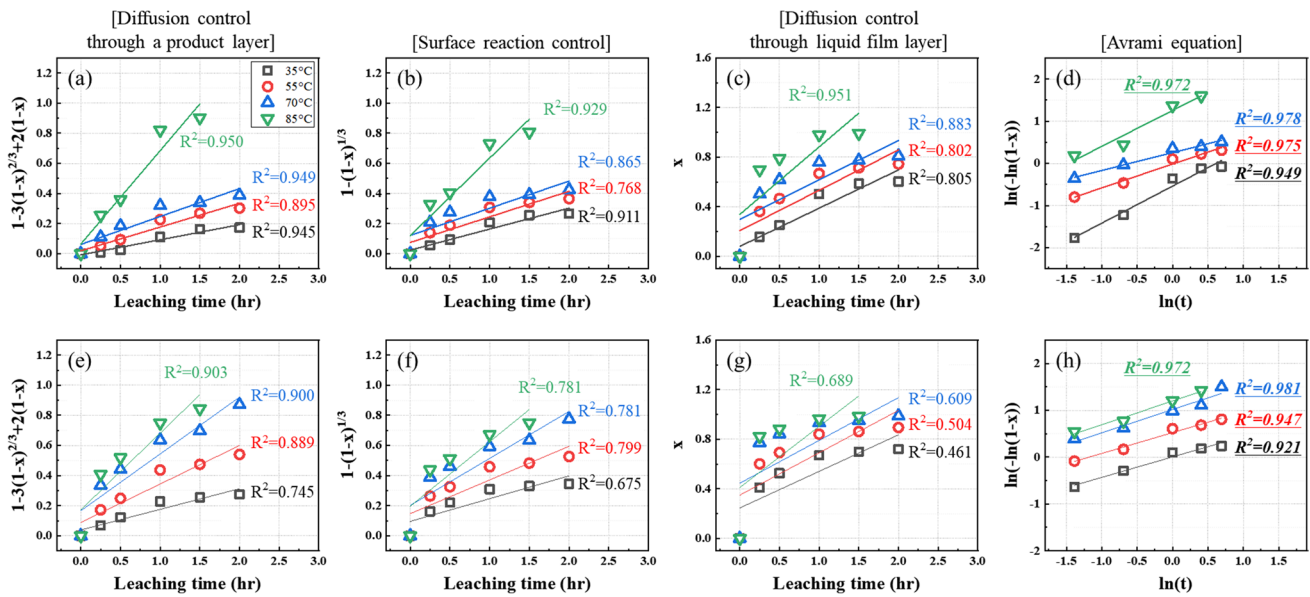
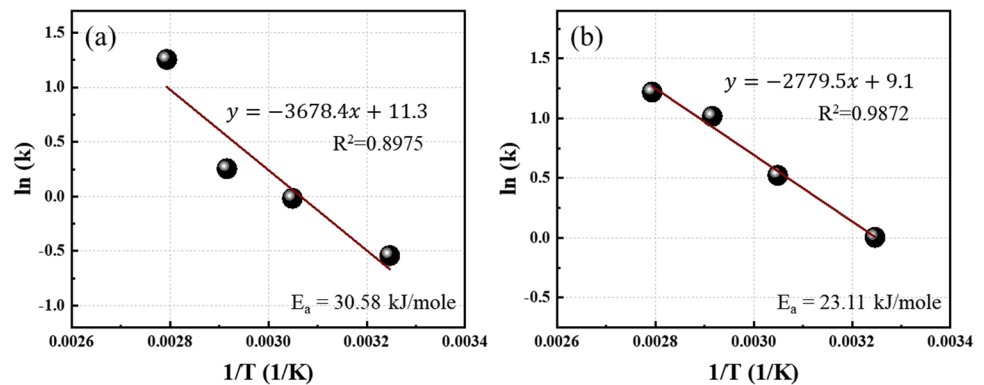


Fig. 4 The linearly fitting results based on four leaching kinetic models: **a–d** Co, **e–h** Li, **a, e** diffusion control through a product layer, **b, f** surface reaction control, **c, g** diffusion control through liquid film layer, **d, h** Avrami equation model

Fig. 5 Arrhenius plot for **a** Co and **b** Li leaching in 2.4M MSA-1.6M CA system



influenced by both the chemical processes and the diffusion of reactants [41, 42]. Therefore, the rate-determining step in the MSA-CA hybrid organic leaching system was determined as the mixed-controlled mechanism which combines surface chemical reaction and liquid film diffusion-controlled mechanism.

3.3 Effect of High S/L Ratio and Lixiviant Concentration

Figure 6 shows the effect of the S/L ratio on the 2.4M MSA-1.6M CA-x vol% H₂O₂ (x=1, 1.25, 1.5, 2 vol%) leaching system. Three tests at 85°C were performed to verify reproducibility. In these tests, considering that the optimized ratio between the S/L ratio and H₂O₂ concentration was 80 g/L:1.0 vol% as shown in Fig. 2, the proportional amount of H₂O₂ was added as the S/L ratio increased. Moreover, H₂O₂ was added in two separate additions. In Fig. 6, the

vol% values above data symbols indicate the added H₂O₂ concentration for each test. The leaching efficiencies of Co and Li in the absence of H₂O₂ were decreased with increasing the S/L ratio. On the other hand, the leaching efficiencies of Co and Li in the presence of H₂O₂ were kept at around 92% despite the increase in the S/L ratio to 120 g/L. At 160 g/L, the leaching efficiencies of Co and Li were decreased; particularly, the decrease of Co leaching was prominent. This result may be due to the crystallization of Co and/or Li ions into compounds of purple color during the leaching test, as shown in Fig. 6. When more than 120 g/L of the LCO was dissolved into the 2.4M MSA-1.6M CA solution, it is believed that the concentration of dissolved Co and/or Li reached the solubility limit during the experiment. The 120 g/L could be concluded as the optimal S/L ratio for the LCO leaching using 2.4M MSA-1.6M CA-1.5vol% H₂O₂ at 85 °C for 60 min. The 120 g/L S/L ratio is an excellent value compared to the previous research on LCO leaching

using organic acids as presented in Table S2 of the supporting information. Furthermore, it is also comparable to the $\text{H}_2\text{SO}_4\text{-H}_2\text{O}_2$ conventional leaching system (100–150 g/L S/L ratio, Table S2) although the Co and Li leaching efficiencies for the MSA-CA- H_2O_2 leaching system were slightly lower than those for the conventional leaching system. The higher S/L ratio achieved in this study is expected to reduce the reagent consumption and the cost. Furthermore, it is believed that the high Co and Li concentration in leachate can facilitate the subsequent Co and Li recovery processes.

3.4 Comparison of Reagent Cost and Electricity Cost

To objectively compare the MSA-CA- H_2O_2 system to various organic leaching systems in terms of economical perspective, the reagent cost per extracted LCO weight and the leaching process cost per extracted LCO weight were calculated based on Eqs. (8) and (9), respectively.

$$\begin{aligned} & \text{reagent cost per extracted LCO weight (\$/kg)} \\ &= \frac{\text{reagent cost for the optimized concentration (\$/L)}}{\text{leached S-L ratio (kg/L)}} \\ &= \frac{\text{reagent cost for the optimized concentration (\$/L)}}{\text{S-L ratio (kg/L)} \cdot (\text{Li E.E. (\%)/100}) \cdot (\text{Co E.E. (\%)/100})} \end{aligned} \quad (8)$$

$$\begin{aligned} & \text{leaching process cost per extracted LCO weight (\$/kg)} \\ &= \frac{[\text{Electricity consumption for heating 1L water (kwh/L)} \cdot \text{electricity rate (\$/kwh)}]}{\text{leached S-L ratio (kg/L)}} \\ &= \frac{\text{Electricity cost for heating 1L lixiviant (\$/L)}}{\text{S-L ratio (kg/L)} \cdot (\text{Li E.E. (\%)/100}) \cdot (\text{Co E.E. (\%)/100})} \end{aligned} \quad (9)$$

Basically, the optimized leaching parameters in the previous studies and this study, such as the S/L ratio, leaching time, and leaching temperature, were summarized in Table S2 of the supporting information to calculate reagent costs per extracted LCO weight (\$/kg) and leaching process costs per extracted LCO weight (\$/kg).

In Eq. (8), the reagent costs used for the optimized concentrations in each leaching system were calculated based on the reagent costs (\$/kg) referred from Sigma-Aldrich, as presented in Table S3 of the supporting information. The calculated reagent costs used for the optimized concentrations were summarized in Table S2 of the supporting information. Meanwhile, the reagent costs (\$/L) used for the optimized concentrations were divided by the leached S/L ratio (kg/L) to determine the reagent cost per extract LCO weight (\$/kg). Here, the leached S/L ratio (kg/L) means the weight of solids leached in the 1L lixiviant according to the Li extraction efficiency (Li E.E., %) and Co extraction efficiencies (Co E.E., %).

For calculating the leaching process cost depending on the temperature and time (Eq. (9)), the electricity consumption of the leaching instrument was measured using a Power Meter in this study. The water of 1L was identically used for this measurement. Figure S1 (a) and (b) of supporting

materials show the measured temperature ($^{\circ}\text{C}$) and the electricity consumption (kWh) for heating 1 L water with the increase in the leaching time. The corresponding electricity cost for heating 1 L water (\$/L) at a specific temperature and specific time was calculated by reflecting the electricity rate of the state of Colorado (0.15 \$/kWh), as shown in Fig. S3 (c). Here, the electricity cost for heating the 1 L water was assumed to be identical to the electricity cost for heating the 1L lixiviant of each organic acid leaching system. Consequently, the electricity costs for heating the 1 L lixiviant could be determined based on the calculated cost data of Fig. S1 (c) and the optimized leaching temperature and time in Table S2. All the calculated values were presented in Table S2 of the supporting information. Meanwhile, the electricity costs (\$/L) were divided by the leached S/L ratio (kg/L) to determine the electricity costs per extract LCO weight (\$/kg).

Figure 7 shows the reagent cost per extracted LCO weight (\$/kg) and the leaching process cost per extracted LCO weight (\$/kg) of various organic leaching systems. The MSA-CA- H_2O_2 leaching system investigated in this study was one of the most effective organic leaching system in terms of economical perspectives. It is believed to be due to the highest S/L ratio although the actual reagent cost is higher than others.

3.5 Leaching Test Using Cathode Scrap from Spent LIBs

The optimal leaching condition was applied for various cathode scrap from spent LIBs for the sake of examination on the diverse applicability of MSA-CA- H_2O_2 leaching system. The leaching conditions were 2.4M MSA, 1.6M CA, 1 vol% H_2O_2 , 80 g/L S/L ratio, 85°C , and 1 h. Figure 8 and Table 3 show the leaching results on two LCO scraps, synthetic NMC622, NMC811 scrap, and NCO scrap. The metal elements of cathode materials were leached above almost 90% under the optimal condition although the leaching efficiencies of one component were slightly lower for the cathode materials containing Ni and/or Mn. For the synthetic NMC622, the leaching efficiency of Mn was 86%. The molar mass of NMCs tends to be lower than that of the LCO. When the S/L ratios were the same, the molar concentration of NMCs is higher than that of the LCO. Therefore, the leaching efficiency of one element might be relatively low. This could be improved by increasing the leaching time or reducing the S/L ratio. In the case of the NMC811 and LNCO scraps, 89% of Ni and 88% of Co were leached. The scraps obtained from spent batteries might contain the electrolyte and/or organic binders which have been known to reduce the leaching kinetics [43]. Thus, to improve the leaching efficiency and rate, it is believed that the pre-treatment for removing the

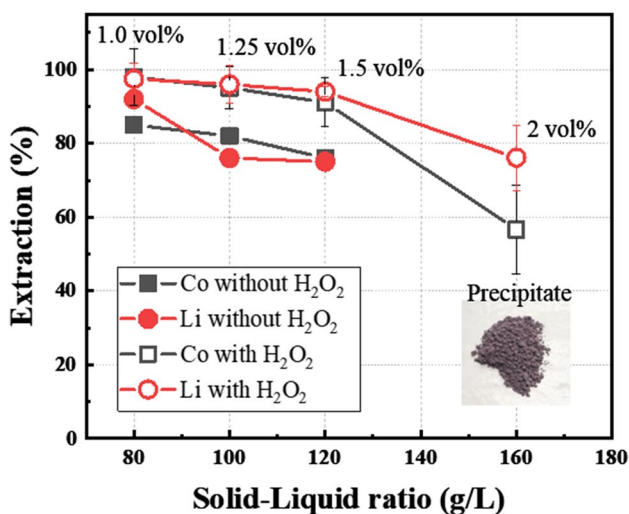


Fig. 6 Effect of S/L ratio on Co and Li extraction in an optimized 2.4 M MSA-1.6 M CA-x vol% H₂O₂ leaching system (x: 1–2 vol%, temperature: 85°C, leaching time: 1 h with H₂O₂ or 6 h without H₂O₂). In the graphs, the vol% value refers to the added H₂O₂ concentration in each test. H₂O₂ was added in two separate additions. The figure on the right shows the purple-colored compound precipitated during the LCO at an S/L ratio of 160 g/L

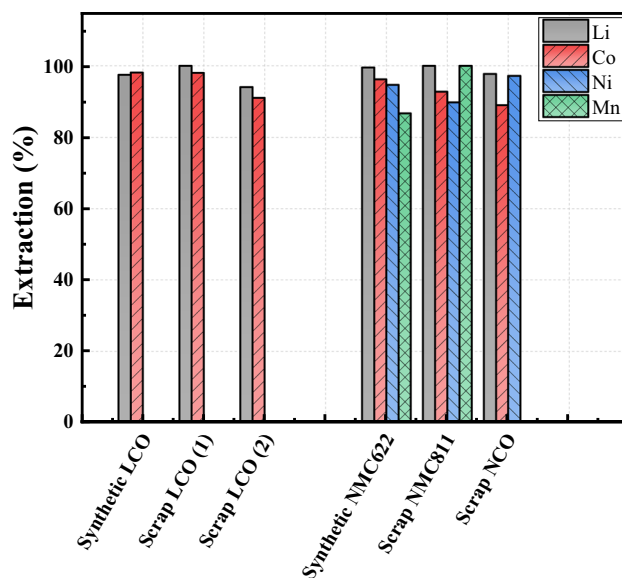


Fig. 8 Leaching results on two LCO scraps, synthetic NMC622, NMC811 scrap, and NCO scrap in the optimized leaching conditions

electrolyte and/or organic binders, such as thermal treatment, must be conducted. Additionally, the lixiviants and/or reductants might be consumed to co-extract the impurities in the scraps such as Al, Cu, and Fe (Table 1). This undesired consumption of lixiviants might make worse the leaching performance of lixiviants. Although the effects

of the impurities or the pre-treatment for removing the electrolyte and/or organic binders on the real battery scrap leaching must be further investigated, it could be confirmed that the MSA-CA mixed leaching system with H₂O₂ could be successfully applied for the various cathode scraps through the applicability tests.

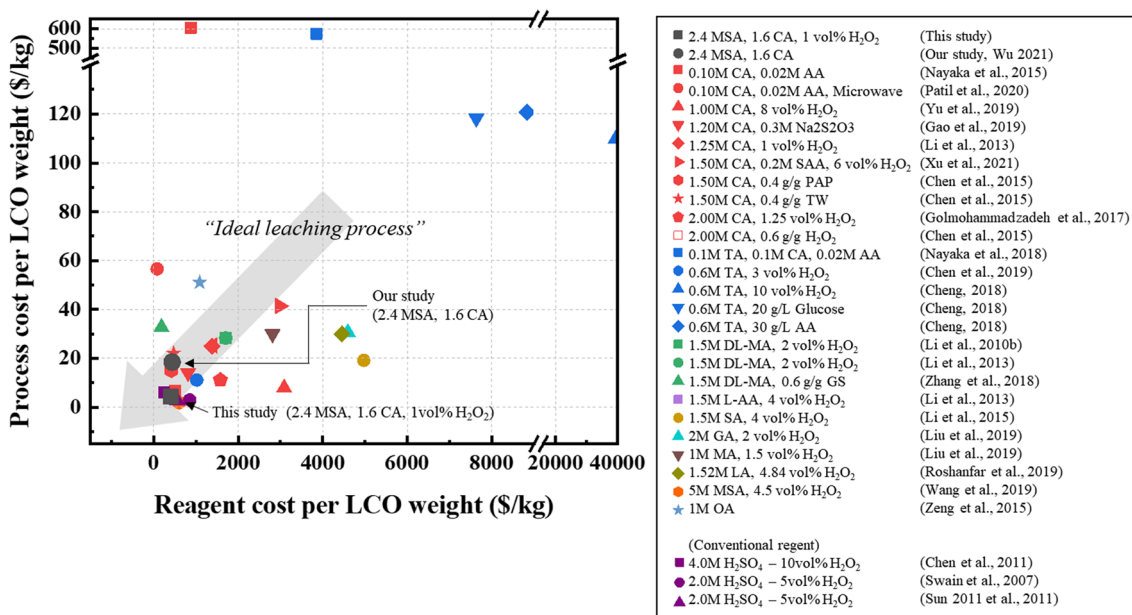


Fig. 7 Reagent cost per extracted LCO weight (\$/kg) and the leaching process cost per extracted LCO weight (\$/kg) of various organic acid based leaching processes

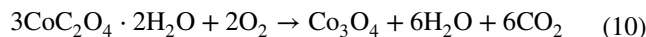
Table 3 Extraction efficiencies on two LCO scraps, synthetic NMC622, NMC811 scrap, and NCO scrap in the optimized leaching conditions

Type of material	Extraction (%)			
	Li	Co	Ni	Mn
Synthetic LCO	97.5	98.1	-	-
Scrap LCO (1)	99.5	98.0	-	-
Scrap LCO (2)	94.0	91.2	-	-
Synthetic NMC622	99.5	96.2	94.6	86.7
Scrap NMC811	100	92.7	89.8	100
Scrap NCO	97.6	88.9	97.2	-

3.6 Co recovery and LCO Regeneration

Figure 9 shows the SEM images and XRD pattern of the recovered CoC_2O_4 precipitates, Co_3O_4 , and regenerated LCO. The MSA-CA leachates obtained from the test using synthetic LCO was used for the Co and Li recovery tests. From the MSA-CA leachate containing Co and Li ions, the Co ions of 99% were selectively recovered into pink-colored CoC_2O_4 with a columnar morphology of about 2 μm in length. The crystallographic phase of the Co precipitates was confirmed to be either crystalline cobalt oxalate dihydrate or cobalt oxalate as shown in the XRD pattern (Fig. 9). The selective recovery of Co is attributed to the higher value of pK_{sp} (i.e., solubility product constants) of CoC_2O_4 ($\text{pK}_{\text{sp,Co}} : 7.2$) than that of $\text{Li}_2\text{C}_2\text{O}_4$ ($\text{pK}_{\text{sp,Li}} : 1.9$) [23, 26]. The high recovery efficiency of 99 % in this study is comparable or superior to previous studies in Table S1 of supporting materials. To generate the cobalt oxide as a precursor of cathode materials, the CoC_2O_4 was calcinated at 400°C for 6 h. Crystallographic phase of the

calcinated precipitates was confirmed to be cobalt (II, III) oxide (Co_3O_4) as shown in the XRD pattern (Fig. 9). The morphology of Co_3O_4 was similar to that of the CoC_2O_4 with columnar structure (Fig. 9). However, their size was slightly decreased to $\sim 1 \mu\text{m}$, and it had mesoporous structure due to the dehydration and loss of oxygen and carbon in the CoC_2O_4 as presented in Eq. (10).



Subsequently, the LCO was regenerated as a cathode material by using the obtained Co_3O_4 and commercial Li_2CO_3 . The Co_3O_4 was homogeneously mixed with commercial Li_2CO_3 using ball milling and the mixture was sintered at 800°C for 15 h in air atmosphere. As shown in Fig. 9, the nano-sized LCO could be regenerated without unreacted Co_3O_4 or Li_2CO_3 .

3.7 Li recovery and LFP Regeneration

The Li ions in leachate were recovered into Li_3PO_4 form using Na_2HPO_4 . To optimize the Li precipitation parameters in the MSA-CA system, the effects of temperature and pH were investigated as shown in Fig. 10 (a). The pH of the leachate was adjusted up to 12 using NaOH and then 0.5 M Na_2HPO_4 solution was added to the leachate with the 1:0.6 molar ratio between Li^+ and PO_4^{3-} ions. The pH value of 0.5M Na_2HPO_4 was around 8 when it was dissolved without any pH control. The precipitation reaction was conducted for 30 min. The SEM images inserted in Fig. 10 (a) show the morphologies obtained at specific recovery conditions. The Li precipitation efficiencies reached up to 97% at 80°C and pH 11. Crystallographic phase of the Li precipitates was confirmed to be Li_3PO_4 as shown in the XRD pattern

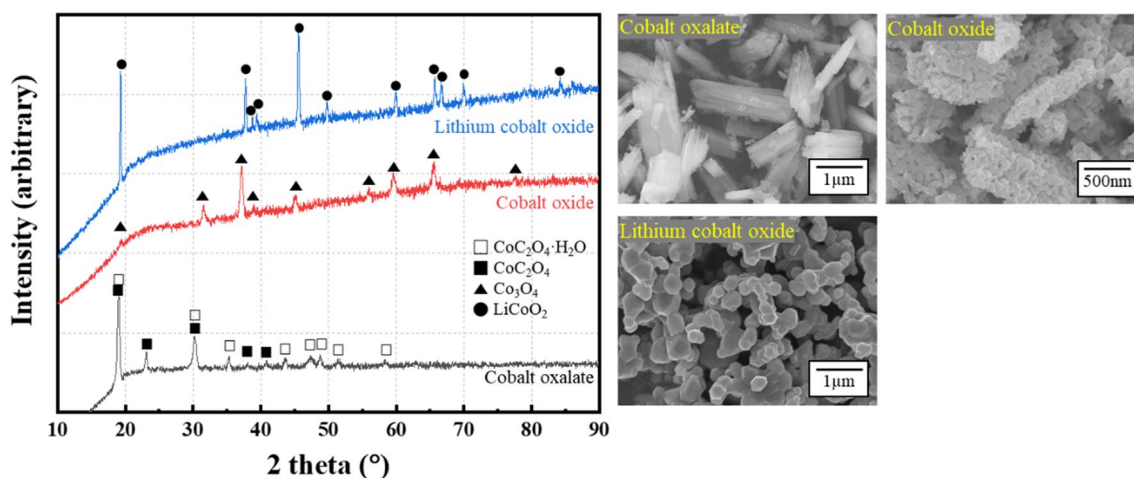


Fig. 9 The SEM images and XRD pattern of the recovered CoC_2O_4 precipitates, Co_3O_4 , and regenerated LCO

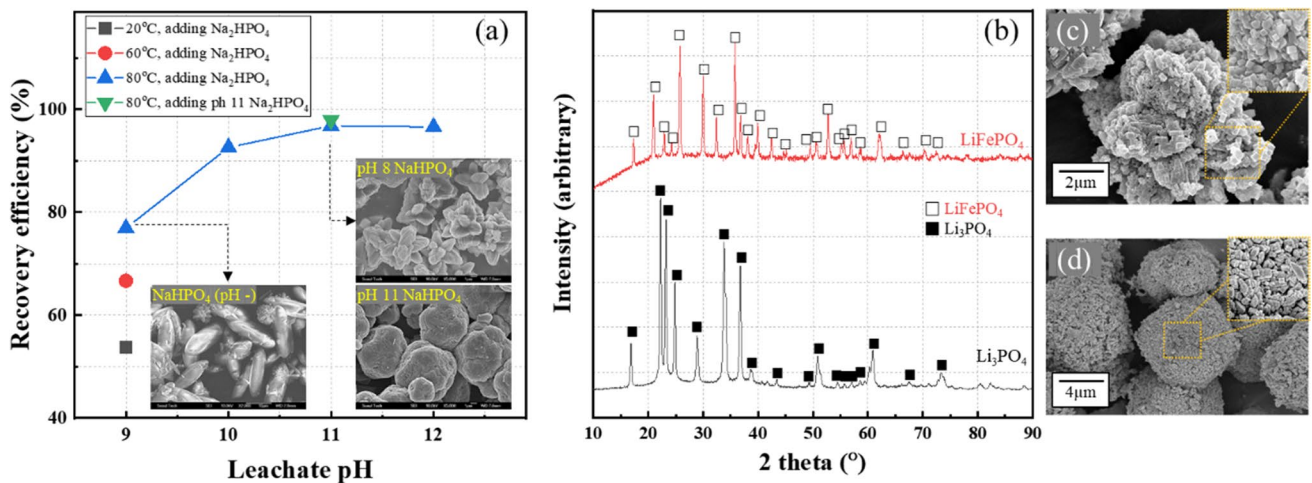


Fig. 10 a Effects of temperature and pH on the Li recovery; b the XRD diffraction patterns of recovered Li₃PO₄ and LFP; SEM images of c flower-like shaped and d sphere-shaped LFP particle

(Fig. 10 (b)). The achieved precipitation efficiency in this study, 97%, is superior to the previous studies: 93% from the spent LIBs leachate [44], 93% from the CA leachate [23], 95.8% from the leaching liquor of mixed type spent LIBs [45], and 98.4% from the H₂SO₄ leaching solution [46]. The recovered Li₃PO₄ was utilized to synthesize the LFP cathode materials via the hydrothermal method. The XRD and SEM analysis results of Fig. 10 (b–d) show that the micro-sized LFPs composed of nano-sized primary particles could be generated as a final product from MSA-CA leachate.

Meanwhile, it was observed that the morphology of recovered Li₃PO₄ was dependent on the recovery conditions.

At the lower pH, Li₃PO₄ of ellipsoid shape with a size of ~10 μm was precipitated. Interestingly, at pH 11, the lithium recovery efficiency was identical (about 97%), but the morphology changed in response to the pH of the added Na₂HPO₄ solution. When the 0.5M Na₂HPO₄ solution with pH 8 was added, flower-like shaped Li₃PO₄ was obtained. On the other hand, the addition of the 0.5M Na₂HPO₄ solution adjusted to pH 11 precipitated the spherite Li₃PO₄. The morphologies of recovered Li₃PO₄ affected that of LFP synthesized by the hydrothermal method. As shown in Fig. 10 (c, d), the overall shape of LFP was maintained after the hydrothermal reactions. The morphology of LFP cathode

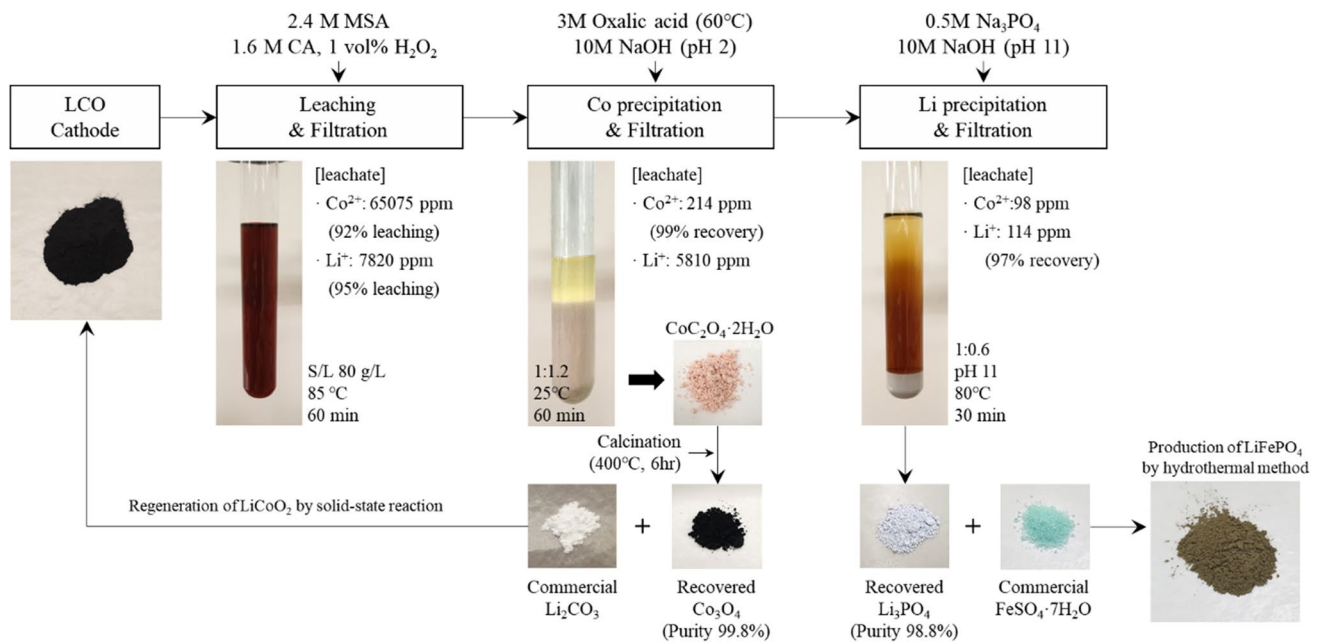


Fig. 11 Flowchart of the recycling process of LCO, which was proposed in this study

materials has been known as one of the important microstructure factors critically affecting the electrochemical performance of LIBs as well as the mechanical stability of cathode materials related to the capacity stability [47–49]. Basically, the inherent physical properties, such as the tab density and surface area, were determined based on the morphology of secondary particles. If the tab density and surface area of cathode particles are increased, the charge/discharge capacity and the Li^+ ion mobility between LiFePO_4 particles and the electrolyte would be improved. Therefore, it is imperative to recover the Li_3PO_4 precursor into optimal morphology high surface area and high tab density to regenerate the LFP with high electrochemical performance. In this perspective, the recovery conditions achieving high recovery efficiency as well as optimal morphology have to be investigated further. The evaluation of the relationship between the electrochemical performance and morphologies of regenerated LFP may be required in future research.

Figure 11 is the proposed flowchart showing the recycling procedure of LCO consisting of leaching, precipitation and regeneration processes in MSA-CA- H_2O_2 system. The MSA-CA- H_2O_2 leaching system showed the outstanding results in terms of Co and Li leaching efficiencies and economical perspective compared to other organic leaching system. The 99 % of Co and 97% of Li could be recovered successfully from the MSA based leaching system. By utilizing the recovered materials, the LCO and LFP could be successfully regenerated.

4 Conclusions

A novel green hydrometallurgical process for LCO recycling using MSA-CA- H_2O_2 mixed organic leaching system was investigated in this study. Co 98% and Li 97 % were leached in the optimized condition; 2.4M MSA, 1.6M CA, 1.0 vol% H_2O_2 , S/L ratio 80 g/L, 85 °C, and 1 h. The LCO dissolution behavior in MSA-CA- H_2O_2 leaching system is well-explained via the Avrami equation. The experimental activation energy of Co and Li was 30.58 kJ/mol and 23.11 kJ/mol, respectively, demonstrating it is the mixed controlled mechanism which combines surface chemical reaction and liquid film diffusion-controlled mechanism. The optimal leaching condition of the MSA-CA- H_2O_2 mixed leaching system exhibited good adaptability to LCO scrap, synthetic NMC622, NMC scrap, and LNCO scrap. The metal elements of various cathode scraps were leached over 90% under the optimal conditions. The dissolved Co and Li ions in the MSA-CA leachate were selectively recovered with high recovery efficiency, 99 % and 97 %, as Co_3O_4 and Li_3PO_4 , respectively. The LCO and LFP were successfully reproduced by using the recovered Co_3O_4 and Li_3PO_4 through solid-state reaction and hydrothermal method. The

economics of the MSA-CA- H_2O_2 leaching system were still not comparable to conventional leaching systems. However, the MSA-CA- H_2O_2 leaching system investigated in this study was one of the most effective organic leaching systems in terms of metal extraction efficiencies and economic perspectives compared to various organic leaching systems.

Supplementary Information The online version contains supplementary material available at <https://doi.org/10.1007/s42461-023-00837-8>.

Acknowledgements Data from this manuscript had been presented in the Symposium in Honor of Patrick R. Taylor at the MINEXCHANGE 2023 SME Annual Conference & Expo, held in Denver, CO, February 26 to March 1, 2023.

Declarations

Conflict of Interest The authors declare no competing interests.

References

1. Gil-Alana LA, Monge M (2019) Lithium: production and estimated consumption. Evidence of persistence. *Resources Policy* 60:198–202
2. Reddy TB, Linden D (2011) *Linden's Handbook of Batteries*, 4th edn. McGraw-Hill Professional Publishing
3. Asadi Dalini E, Karimi G, Zandevakili S, Goodarzi M (2020) A review on environmental, economic and hydrometallurgical processes of recycling spent lithium-ion batteries. *Miner Process Extr Metall Rev* 42(7):451–472
4. Liu Y, Xing P, Liu J (2017) Environmental performance evaluation of different municipal solid waste management scenarios in China. *Resources, Conservation and Recycling* 125:98–106
5. Xie R, Zhu Y, Liu J, Li Y, Wang X, Shumin Z (2020) Research status of spodumene flotation: a review. *Mineral Processing and Extractive Metallurgy Review* 42(5):321–334
6. Engel H, Hertzke P, Siccardo G (2019) Second-life EV batteries: the newest value pool in energy storage. McKinsey & Company
7. Choi Y, Rhee SW (2020) Current status and perspectives on recycling of end-of-life battery of electric vehicle in Korea (Republic of). *Waste Manag* 106:261–270
8. Sommerville R, Zhu P, Rajaeifar MA, Heidrich O, Goodship V, Kendrick E (2021) A qualitative assessment of lithium ion battery recycling processes. *Resources, Conservation and Recycling* 165:105219
9. Okonkwo EG, Wheatley G, He Y (2021) The role of organic compounds in the recovery of valuable metals from primary and secondary sources: a mini-review. *Resources, Conservation and Recycling* 174:105813
10. Lv W, Wang Z, Cao H, Sun Y, Zhang Y, Sun Z (2018) A critical review and analysis on the recycling of spent lithium-ion batteries. *ACS Sustainable Chemistry & Engineering* 6(2):1504–1521
11. Jha MK, Kumari A, Jha AK, Kumar V, Hait J, Pandey BD (2013) Recovery of lithium and cobalt from waste lithium ion batteries of mobile phone. *Waste Manag* 33(9):1890–1897
12. Chen X, Ma H, Luo C, Zhou T (2017) Recovery of valuable metals from waste cathode materials of spent lithium-ion batteries using mild phosphoric acid. *J Hazard Mater* 326:77–86
13. Peng C, Hamuyuni J, Wilson BP, Lundstrom M (2018) Selective reductive leaching of cobalt and lithium from industrially crushed waste Li-ion batteries in sulfuric acid system. *Waste Manag* 76:582–590

14. Wang B, Lin XY, Tang Y, Wang Q, Leung MK, Lu XY (2019) Recycling LiCoO₂ with methanesulfonic acid for regeneration of lithium-ion battery electrode materials. *J Power Sources* 436:226828
15. Fu Y, He Y, Qu L, Feng Y, Li J, Liu J, Zhang G, Xie W (2019b) Enhancement in leaching process of lithium and cobalt from spent lithium-ion batteries using benzenesulfonic acid system. *Waste Manag* 88:191–199
16. Gao W, Liu C, Cao H, Zheng X, Lin X, Wang H, Zhang Y, Sun Z (2018) Comprehensive evaluation on effective leaching of critical metals from spent lithium-ion batteries. *Waste Manag* 75:477–485
17. Golmohammadzadeh R, Rashchi F, Vahidi E (2017) Recovery of lithium and cobalt from spent lithium-ion batteries using organic acids: process optimization and kinetic aspects. *Waste Manag* 64:244–254
18. Li L, Dunn JB, Zhang XX, Gaines L, Chen RJ, Wu F, Amine K (2013) Recovery of metals from spent lithium-ion batteries with organic acids as leaching reagents and environmental assessment. *J Power Sources* 233:180–189
19. Li L, Qu W, Zhang X, Lu J, Chen R, Wu F, Amine K (2015) Succinic acid-based leaching system: a sustainable process for recovery of valuable metals from spent Li-ion batteries. *J Power Sources* 282:544–551
20. Meng Q, Zhang Y, Dong P (2017) Use of glucose as reductant to recover Co from spent lithium ions batteries. *Waste Manag* 64:214–218
21. Zhang Y, Meng Q, Dong P, Duan J, Lin Y (2018) Use of grape seed as reductant for leaching of cobalt from spent lithium-ion batteries. *Journal of Industrial and Engineering Chemistry* 66:86–93
22. Wu Z, Soh T, Chan JJ, Meng S, Meyer D, Srinivasan M, Tay CY (2020b) Repurposing of fruit peel waste as a green reductant for recycling of spent lithium-ion batteries. *Environ Sci Technol* 54(15):9681–9692
23. Chen X, Luo C, Zhang J, Kong J, Zhou T (2015a) Sustainable recovery of metals from spent lithium-ion batteries: a green process. *ACS Sustain Chem Eng* 3(12):3104–3113
24. Golmohammadzadeh R, Faraji F, Rashchi F (2018) Recovery of lithium and cobalt from spent lithium ion batteries (LIBs) using organic acids as leaching reagents: a review. *Resour Conserv Recycl* 136:418–435
25. Xu M, Kang S, Jiang F, Yan X, Zhu Z, Zhao Q, Teng Y, Wang Y (2021) A process of leaching recovery for cobalt and lithium from spent lithium-ion batteries by citric acid and salicylic acid. *RSC Adv* 11(44):27689–27700
26. Chen X, Fan B, Xu L, Zhou T, Kong J (2016) An atom-economic process for the recovery of high value-added metals from spent lithium-ion batteries. *J Clean Prod* 112:3562–3570
27. Meng F, Liu Q, Kim R, Wang J, Liu G, Ghahreman A (2020) Selective recovery of valuable metals from industrial waste lithium-ion batteries using citric acid under reductive conditions: leaching optimization and kinetic analysis. *Hydrometallurgy* 191:105160
28. Fu Y, He Y, Chen H, Ye C, Lu Q, Li R, Xie W, Wang J (2019a) Effective leaching and extraction of valuable metals from electrode material of spent lithium-ion batteries using mixed organic acids leachant. *J Ind Eng Chem* 79:154–162
29. Nayaka GP, Zhang Y, Dong P, Wang D, Pai KV, Manjanna J, Santhosh G, Duan J, Zhou Z, Xiao J (2018) Effective and environmentally friendly recycling process designed for LiCoO₂ cathode powders of spent Li-ion batteries using mixture of mild organic acids. *Waste Manag* 78:51–57
30. Ahn J, Wu J, Lee J (2019) Investigation on chalcopyrite leaching with methanesulfonic acid (MSA) and hydrogen peroxide. *Hydrometallurgy* 187:54–62
31. Gernon MD, Wu M, Buszta T, Janney P (1999) Environmental benefits of methanesulfonic acid: comparative properties and advantages. *Green Chem* 1:127–140
32. Wu J, Ahn J, Lee J (2020a) Kinetic and mechanism studies using shrinking core model for copper leaching from chalcopyrite in methanesulfonic acid with hydrogen peroxide. *Mineral Processing and Extractive Metallurgy Review* 42(1):38–45
33. Wu Z, Dreisinger DB, Urch H, Fassbender S (2014) Fundamental study of lead recovery from cerussite concentrate with methanesulfonic acid (MSA). *Hydrometallurgy* 142:23–35
34. Li L, Ge J, Wu F, Chen R, Chen S, Wu B (2010b) Recovery of cobalt and lithium from spent lithium ion batteries using organic citric acid as leachant. *J Hazard Mater* 176(1-3):288–293
35. Zhao Y, Yuan X, Jiang L, Wen J, Wang H, Guan R, Zhang J, Zeng G (2020) Regeneration and reutilization of cathode materials from spent lithium-ion batteries. *Chem Eng J* 383:123089
36. Wu J (2021) Application of green lixivants in metal extraction from primary and secondary metal resources” (Doctoral dissertation,. The University of Arizona)
37. Vanysek P (2000) Electrochemical series. *CRC handbook of chemistry and physics* 8:8–33
38. Zhang X, Cao H, Xie Y, Ning P, An H, You H, Nawaz F (2015) A closed-loop process for recycling LiNi_{1/3}Co_{1/3}Mn_{1/3}O₂ from the cathode scraps of lithium-ion batteries: process optimization and kinetics analysis. *Sep Purif Technol* 150:186–195
39. Zhuang L, Sun C, Zhou T, Li H, Dai A (2019) Recovery of valuable metals from LiNi_{0.5}Co_{0.2}Mn_{0.3}O₂ cathode materials of spent Li-ion batteries using mild mixed acid as leachant. *Waste Manag* 85:175–185
40. Sokić MD, Marković B, Živković D (2009) Kinetics of chalcopyrite leaching by sodium nitrate in sulphuric acid. *Hydrometallurgy* 95(3-4):273–279
41. Habashi F (1999) Kinetics of metallurgical processes. *Métallurgie Extractive Québec*. Québec, QC, Canada
42. Shi G, Liao Y, Su B, Zhang Y, Wang W, Xi J (2020) Kinetics of copper extraction from copper smelting slag by pressure oxidative leaching with sulfuric acid. *Sep Purif Technol* 241:116699
43. Kim S, Bang J, Yoo J, Shin Y, Bae J, Jeong J, Kim K, Dong P, Kwon K (2021) A comprehensive review on the pretreatment process in lithium-ion battery recycling. *J Clean Prod* 294:126329
44. Song Y, Zhao Z (2018) Recovery of lithium from spent lithium-ion batteries using precipitation and electro dialysis techniques. *Sep Purif Technol* 206:335–342
45. Chen X, Xu B, Zhou T, Liu D, Hu H, Fan S (2015b) Separation and recovery of metal values from leaching liquor of mixed-type of spent lithium-ion batteries. *Sep Purif Technol* 144:197–205
46. Shin DJ, Joo SH, Lee D, Shin SM (2022) Precipitation of lithium phosphate from lithium solution by using sodium phosphate. *Can J Chem Eng* 2022:1–8
47. Bao L, Xu G, Wang M (2019) Controllable synthesis and morphology evolution of hierarchical LiFePO₄ cathode materials for Li-ion batteries. *Mater Charact* 157:109927
48. Ma Z, Shao G, Fan Y, Wang G, Song J, Liu T (2014) Tunable morphology synthesis of LiFePO₄ nanoparticles as cathode materials for lithium ion batteries. *ACS Appl Mater Interfaces* 6(12):9236–9244
49. Robinson JP, Koenig GM Jr (2015) Tuning solution chemistry for morphology control of lithium-ion battery precursor particles. *Powder Technol* 284:225–230

Publisher's Note Springer Nature remains neutral with regard to jurisdictional claims in published maps and institutional affiliations.

Springer Nature or its licensor (e.g. a society or other partner) holds exclusive rights to this article under a publishing agreement with the author(s) or other rightsholder(s); author self-archiving of the accepted manuscript version of this article is solely governed by the terms of such publishing agreement and applicable law.